JOURNAL OF CATALYSIS **178,** 555–565 (1998)
ARTICLE NO. CA982196

Characterization of Acidic Sites of Silica-Supported Transition Metal Sulfides by Pyridine and 2,6 Dimethylpyridine Adsorption: Relation to Activity in CH_3SH Condensation

Gilles Berhault,* Michel Lacroix,*,[1] Michèle Breysse,*,[2] Françoise Maugé,† Jean-Claude Lavalley,† Hong Nie,‡ and Lianglong Qu‡

*Institut de Recherches sur la Catalyse, 2, Avenue Albert Einstein, 69626 Villeurbanne Cedex, France; †Laboratoire Catalyse et Spectrochimie, ISMRA-Université, 6, Boulevard du Maréchal Juin, 14050 Caen Cedex, France; and ‡Research Institute of Petroleum Processing, 18 Xueyuan Road, P.O. Box 914, Beijing 100083, China

Received February 9, 1998; revised June 5, 1998; accepted June 5, 1998

The modification of the Brønsted and Lewis acidity induced by a reductive hydrogen treatment has been investigated on three silica supported sulfides, i.e. RuS_2, MoS_2, and a Co-promoted molybdenum sulfide. The catalytic properties of various reduced surfaces have been determined using a model acid demanding reaction such as the condensation of methylmercaptan into dimethylthioether. The acidic properties of the reduced solid were studied by FTIR spectroscopy using both pyridine and 2, 6 dimethylpyridine as probe molecules. Results show that these catalysts present distinct reactivities and stabilities towards a hydrogen atmosphere. For instance the reducibility of RuS_2 is higher than that of MoS_2. Similarly, the number of Lewis acidic sites is higher on RuS_2 than on MoS_2 and no differences in Lewis acidic strength were detected on both systems. On RuS_2 it is easier to create SH groups than on MoS_2; however, on the latter the SH groups have a higher protonic character than over the Ru-based solid. Concerning the effect of Co, the promoter increases the reducibility of the molybdenum phase, inducing an augmentation of the number of both types of acidic centers. The variation of the activity in CH_3SH condensation is very close to that reported for Lewis acidity. This confirms that methylmercaptan condensation is a suitable reaction to follow acidic properties of sulfided catalysts. This study provides evidence for the sensitivity of surface properties of sulfided catalysts to the reaction conditions. It points out that the reducibility of solids plays an important role since the lower the strength of the M-S bond, the easier the creation of numerous Lewis acidic sites and the higher the activity for a reaction requiring moderate acidity.

INTRODUCTION

Transition metal sulfides (TMS) are widely applied for performing hydrodesulfurization (HDS), hydrodenitrogenation (HDN), as well as hydrogenation reactions. In order to catalyze simultaneously these reactions, TMS generally operate with large excess of hydrogen and at temperatures ranging from 573 to 673K. In these reducing atmospheres the surface of the sulfided phases is reduced by sulfur elimination and the resulting coordinatively unsaturated sites (CUS) were recognized to be of prime importance for explaining the catalytic properties of these systems (1–3). These anionic vacancies are indeed active for the chemisorption of the organic substrates to be transformed because chemisorption of unsaturated hydrocarbons or O, S, and N containing molecules generally proceeds by electron donation to these sulfur vacant sites (4, 5). Accordingly, CUS intervenes as an electron withdrawing site whose properties may be regarded as a Lewis-type center interacting with electrodonating organic substrates (6, 7). In addition to these chemisorbing sites the presence of SH groups was also detected by several physicochemical techniques and it was suggested that they might intervene in catalysis (8–14). Their formation results either from hydrogen reduction of the solid or from heterolytic dissociation of H_2S that is almost always present in the feed during a catalytic run. According to these literature data, the surface of a TMS may possess both Lewis and Brønsted acidic sites whose relative population would be dependent on the temperature and on the composition of the surrounding atmosphere, i.e. hydrogen and H_2S partial pressures.

Chemisorption of small basic molecules such as ammonia, pyridine, and lutidine (2, 6-dimethylpyridine) is often used to probe the acidity of solids (15–18). These molecules interact with acidic sites because they have a lone electron pair at the nitrogen atom available for donation to a Lewis acidic site and because they can accept a proton from Brønsted sites. The infrared spectra of the resulting adsorbed species, i.e. PyL and pyridinium ion PyH^+ are clearly distinct, so that the corresponding surface sites can be easily distinguished using this technique (19–21). Nevertheless,

[1] Corresponding author. E-mail: lacroix@catalyse.univ-lyon1.fr.
[2] Present address: Laboratoire de Réactivité de Surface, Université P. et M. Curie, 4, place Jussieu, Casier 178, 75252 Paris cedex 05, France.

0021-9517/98 $25.00

pyridine interacts both with the support and the sulfided phase and many studies report difficulties in characterizing specifically the weak Lewis and Brønsted acid sites of the sulfided phase. However, Topsøe *et al.* provided evidence for the presence of Brønsted acid sites on the sulfided phase by adsorbing pyridine at high temperatures (22). Furthermore, the utilization of these probe molecules has catalytic relevance in connection with the overall hydrotreatment process for several reasons: i.e., (i) NH_3 is the product in the HDN reaction; (ii) compounds like amines, pyridine, or indole are representative of the HDN process; and (iii) basic compounds typically poison the HDS and hydrogenation reactions (23–24).

Besides these nitrogen-containing probe molecules, the chemisorption of alcohols was also utilized to characterize various metal oxide surfaces. IR spectroscopy has shown that the interaction of alcohols with oxides is sensitive enough to identify the various adsorption modes (25–26). For instance, the $\nu(CH_3)$ vibration of molecularly adsorbed alcohols is characterized by high wavenumbers while dissociative chemisorption forming alkoxy groups leads to low $\nu(CH_3)$ frequencies. According to Knözinger *et al.* (27), the presence of these two sorbed states may account for olefin or ether formation coming from either dehydration or disproportionation of the alcohol used as reactant. For instance, adsorption of MeOH, EtOH, *n*-PrOH, *n*-BuOH, and benzyl alcohol on alumina shows the existence of surface alcoholate structures, i.e. RO^- adsorbed on a Lewis center, and all these alcohols yield to ether formation at quite low reaction temperatures. By contrast, no aluminium alcoholate is formed by the adsorption of cyclohexanol on alumina and cyclohexene is the major product formed in similar experimental conditions. Taking into account pyridine inhibition experiments, these authors concluded that alcoholate engendering is a necessary prerequisite for ether formation. The interaction of C_2H_5SH with an alumina support has been studied by Sugioka *et al.* (28). From IR experiments they showed that thiol chemisorption gave rise to a band at 1268 cm^{-1} ascribed to the vibration $\delta(CH_2)$ of Al-S-C_2H_5 species and to a concomitant broadening of the hydroxyl groups absorption in the range of 3000–3500 cm^{-1}. As the SH vibration of the organic molecule was not observed, they concluded that ethanethiol dissociatively adsorbed at the surface, leading to the formation of OH and thiolate species. Moreover, the authors claimed that these species might be intermediates in the formation of diethylsulfide. Similar data were obtained by several authors (29, 30) for the adsorption of CH_3SH on various oxides with different acid–base properties and they concluded that the most effective catalysts for the formation of dimethylsulfide (DMS) are those containing acid–base centers, namely strong Lewis acidic sites and medium basic sites. Recently, we have also shown that this sulfur-containing molecule dissociates at the surface of a model ruthenium sulfide-based catalyst and we proposed that this molecule could be used for probing the acid–base pairs present at the surface of sulfided materials (31).

Basic research related to the catalytic properties of various metal sulfides has provided interesting opportunities to gain insight into the roles of different types of sites (32–38). Obtained literature data support the view that differences in activities are related to changes in the concentration of anionic vacancies which in turn depend on the metal–sulfur bond strength. Despite this, no detailed information is available up to now concerning the abundance and the acidic properties of the SH groups on TMS. One may expect, however, that their stability and concentration will increase with increasing metal–sulfur bond strength. For these reasons, the aim of this work was to examine the variation of the acidic properties induced by hydrogen reduction of three selected supported systems : ruthenium, molybdenum, and cobalt-promoted molybdenum sulfides. The last was chosen in order to gain more insight into the role of the promoter while the unicomponent systems were chosen because of important differences in their catalytic properties. Concerning the support, silica was used in order to avoid any contribution of the carrier to the acidity of the system. As pyridine well characterizes Lewis acidity and lutidine (2,6-dimethylpyridine) is more sensitive than pyridine for probing Brønsted sites, both molecules were used to probe the surface properties of the sulfides. The catalytic properties were determined using the condensation of methylmercaptan (MeSH) in order to avoid olefin formation and a possible oxidation of the solids with oxygen-containing molecules such as alcohols, ethers, and water.

EXPERIMENTAL

Catalyst Preparation

The silica-supported catalysts were prepared using the pore-filling method. The carrier was a high surface area Grace Davison 432 silica of 300 m^2/g BET area with a pore volume of 0.5 cm^3/g. The silica was dried overnight at 383 K prior to its impregnation with aqueous solutions of the metal salts. $RuCl_3$, xH_2O (from Johnson Matthey) was utilized for the preparation of the Ru-based catalyst while cobalt nitrate and molybdenum heptamolybdate were used for the synthesis of the Mo and CoMo samples. The latter was prepared in one step by coimpregnation of the support. The impregnated solids were then dried at 383 K before their transformation into a sulfided phase. The sulfidation of the Ru-containing catalyst was performed by heating the precursor at 673 K with a 15% H_2S–85% N_2 atmosphere in order to avoid the intermediate formation of a metallic phase that is known to be difficult to sulfide (39) while a mixture of 15% H_2S–85% H_2 was used for the sulfidation of the Mo and CoMo. After this activation procedure, the

solids were cooled to room temperature in the presence of the sulfur-containing atmosphere, flushed with an oxygen-free nitrogen flow, and stored in sealed bottles. The Ru and Mo loading were respectively 7 and 6 wt%. The amount of Co added to the Mo phase was adjusted in order to have Co/(Co + Mo) ratio equals to 0.3. A cobalt supported on a silica catalyst (6 wt% of Co) used as reference sample was prepared from cobalt nitrate and sulfided according to the same procedure as that used for the Mo-based systems.

Catalyst Reduction and Catalytic Activity

Reduction of the catalysts was performed *in situ* in the same flow microreactor as the one used for the determination of the catalytic activity. The unit is connected to a gas chromatograph (HP 5890A) equipped with a flame photometric detector (FPD) and a flame ionization detector (FID). After loading the sample into the reactor, the solid was flushed under nitrogen for 15 min and then contacted with a hydrogen flow of 100 $cm^3 \cdot min^{-1}$ at room temperature. The solid was then reduced by heating the reactor up to the desired temperature using a heating rate of 2 $K \cdot min^{-1}$ and left in isothermal conditions for 2 h. The amount of H_2S released by the solid during the reduction process was quantified by calibrating the FPD detector with a known concentration of H_2S (1153 ppm) diluted in hydrogen. The degree of reduction α was defined by the ratio of the amount of H_2S eliminated from the solid to the total sulfur content.

After an *in situ* reduction, hydrogen was replaced by nitrogen and the reactor temperature was fixed at 473 K. The reduced catalyst was then submitted to a flow (63 $cm^3 \cdot min^{-1}$) of MeSH/N_2. The partial pressure of methylmercaptan (MeSH) was 40 Torr. The analysis of the reaction mixture was performed using a HP-5 capillary column (crosslinked Ph-Me Silicon, 50 m × 0.32 mm × 0.25 μm) maintained at 333 K. Besides the reactant (MeSH), only H_2S and DMS were detected under these experimental conditions. Their retention times are respectively 4.6, 4.3, and 5.5 min. As a FPD detector is extremely sensitive towards sulfur-containing molecules, it was used only to quantify the H_2S production while the hydrocarbons were analyzed using the FID detector. Conversions were kept lower than 10% by adjusting either the catalyst weight or the total flow in order to avoid possible mass transfer limitations.

Electron Microscopy Characterization

High-resolution electron microscopy examinations were performed with a Jeol 100 CX instrument fitted with a UHP polar piece (resolving power = 0.2 nm). After the hydrogen treatment, the reduced solids were immediately immersed into deoxygenated heptane at room temperature in order to prevent their oxidation. Then the samples were ultrasonically dispersed in this solvent and the suspension was collected on a carbon-coated copper grid. Particle size distribution was determined by counting about 500–600 particles. The average particle size was calculated according to the first mode of the distribution:

$$\sum_{i=1}^{n} n_i L_i \Big/ \sum_{i=1}^{n} n_i$$

FTIR Spectroscopy

FTIR characterization of adsorbed probe molecules was performed using self-supporting discs (5 $mg \cdot cm^{-2}$) of pressed samples. As this pelletizing step cannot be done without air exposure, the catalysts were resulfided *in situ* in the infrared transmission cell. For this purpose, the pellet was first evacuated at room temperature and then contacted with 100 Torr of H_2S (15%)-He for the Ru catalyst or of H_2-H_2S (15%) for Mo, Co, and CoMo catalysts. The cell was then heated up to 673 K with a heating rate of 10 $K \cdot min^{-1}$ and maintained at this temperature for 30 min. The sulfidation was followed by an evacuation at 673 K for 30 min. This sulfidation–evacuation procedure was repeated twice and the system was cooled down to room temperature under evacuation before solid reduction. Then 200 Torr of pure hydrogen was introduced in the cell, which was then heated up to the desired reduction temperature. Several reduction–evacuation cycles were done in order to remove the H_2S formed upon reduction. At last, all the samples were evacuated at 393 K for 30 min prior to probe molecule adsorption. The so-treated catalysts were then contacted with 2 Torr of pyridine or 2,6-dimethylpyridine (DMP) at room temperature. In these conditions, preliminary experiments have shown that adsorption reaches an equilibrium rapidly. The solids were then evacuated at room temperature or at 423 K in order to estimate the bond strength between the solid surface and the adsorbate. The IR spectra were recorded using a Nicolet 60SX FTIR spectrometer, either in the presence of the gas phase or after evacuation at room temperature or at 423 K. Band intensities were corrected for slight differences in catalyst weight. The band areas were calculated by integration using the IR Omnic software.

RESULTS

Catalyst Reduction

As the composition of the three catalysts investigated changes according to the severity of the reduction treatment, all the samples will be denoted thereafter by Ru/SiO_2, Mo/SiO_2, and CoMo/SiO_2. Figure 1 represents the variation of the degree of reduction α with the temperature. Among the TMS studied, Ru/SiO_2 appears to be highly reducible since all the sulfur content can be removed by heating the catalyst under hydrogen at a temperature as low as 673 K. By contrast, on Mo/SiO_2, only 25% of the sulfur is released at 1073 K. The addition of cobalt increases the reducibility of the system because a degree of reduction of 100% could

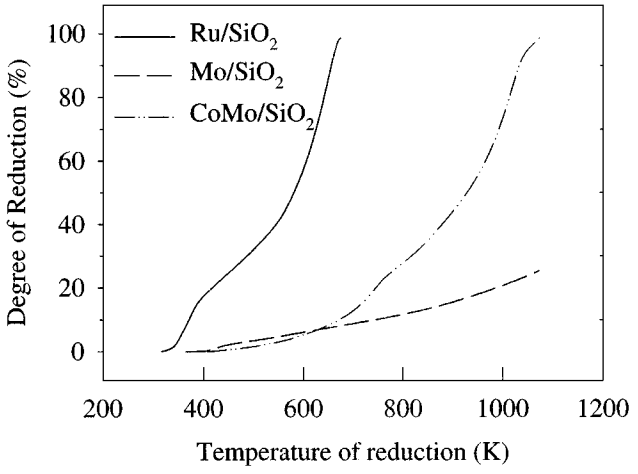

FIG. 1. Variation of the reduction degree α versus the reduction temperature for the three sulfided catalysts : Ru/SiO_2, Mo/SiO_2, and $CoMo/SiO_2$.

be attained at this temperature. Consequently, the three systems exhibit quite different stabilities towards hydrogen treatment and it could be expected that this behavior would induce differences in catalytic and chemisorptive properties.

Catalytic Activities

As shown in Fig. 2, the catalytic properties of the TMS significantly vary, depending on the severity of the reducing pretreatment. For Ru/SiO_2, the nonreduced sample already exhibits a significant catalytic activity towards the transformation of CH_3SH into CH_3SCH_3. This unexpected activity level is related to the presence of the ruthenium phase because the silica support, either sulfided or reduced, does not present any detectable catalytic property. This result shows

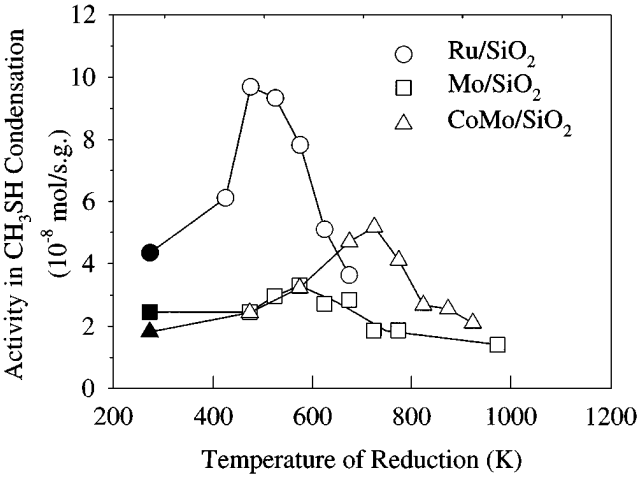

FIG. 2. Activity towards CH_3SH condensation reaction versus of the reduction temperature for the three catalysts : Ru/SiO_2, Mo/SiO_2, and $CoMo/SiO_2$. On all the figures the black filled squares correspond to nonreduced solid.

that the Ru/SiO_2 catalyst already contains some sites able to catalyze this reaction. The activity increases with sulfur removal up to a temperature of reduction of 473 K and then continuously declines for higher reduction temperatures. According to the data reported in Fig. 1, the maximum in activity corresponds to a degree of reduction of about 20%.

Despite the low activity of Mo/SiO_2, a maximum of activity also appears around 573–673K and then goes down when the reduction temperature is further increased. The presence of cobalt shifts the maximum in activity from 573 to 723 K. At the maximum, its activity is higher than the activity of the nonpromoted Mo/SiO_2 and lower than that observed for the ruthenium-containing catalyst.

Electron Microscopy

The morphology of the Ru/SiO_2 particles can be depicted as small spheres dispersed at the surface of the support. As reported in Table 1, the initial and nonreduced sample presents an average particle size of 36 Å. This mean-particle size remains constant up to a reduction temperature of 573 K and then increases due to sintering. Therefore, the observed diminution of the activity at $T_r > 473$ K cannot be ascribed to the sintering of the active phase.

For Mo/SiO_2, only a slight increase of the average particle size and of the mean number of layers was observed, while these parameters are rather constant for the $CoMo/SiO_2$-promoted sample catalyst.

Infrared Spectroscopy of Adsorbed Pyridine

The interaction of pyridine with the sulfided silica support is presented in Fig. 3. The low wavenumber of the pyridine ν_{8a} vibration at 1596 cm^{-1} and the disappearance of bands at 1444, 1485, and 1596 cm^{-1} after evacuation at 323 K show that pyridine interacts by hydrogen bonding. Two weak bands at 1455 and 1625 cm^{-1} are also observed, indicating

TABLE 1

Mean Particle Size Data of Silica-Supported Ru, Mo, and CoMo Sulfides Reduced at Different Temperatures

Catalyst	Reduction temperature (K)	L (Å)	*n*
Ru/SiO_2	none	36	—
Ru/SiO_2	473	37	--
Ru/SiO_2	573	43	--
Ru/SiO_2	633	65	--
Ru/SiO_2	673	110	--
Mo/SiO_2	None	24	2.4
Mo/SiO_2	473	29	2.3
Mo/SiO_2	573	35	2.9
Mo/SiO_2	673	39	2.9
$CoMo/SiO_2$	None	32	2.3
$CoMo/SiO_2$	723	39	2.8
$CoMo/SiO_2$	823	36	2.6

Note. For the Ru catalyst L is the mean diameter while for Mo-based catalysts L denotes the mean slab length and *n* is the number of slabs.

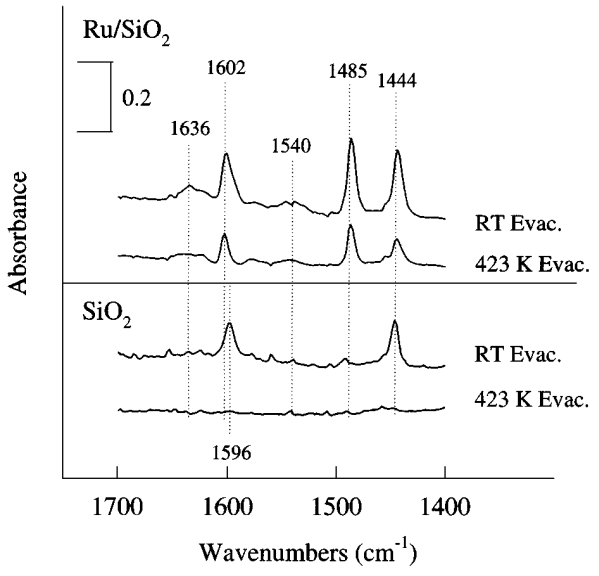

FIG. 3. IR spectra of the species resulting from pyridine evacuation at room temperature and at 423 K on silica support and on silica-supported ruthenium sulfide reduced at 423 K.

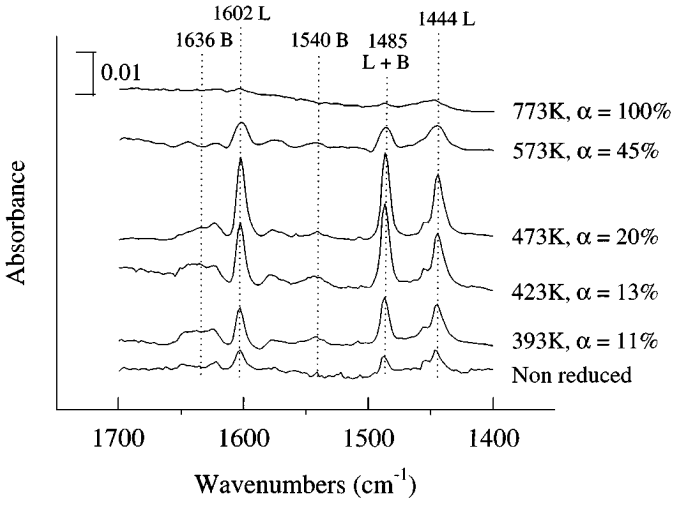

FIG. 4. IR spectra of the species resulting from pyridine evacuation at 423 K on Ru/SiO_2 reduced at various temperatures.

the presence of a small number of strong Lewis acidic sites due to alumina as impurities in the support (1500 ppm).

A different comportment was observed in the presence of a sulfided phase. To illustrate this, Fig. 3 reports, as an example, the data obtained on a Ru-based catalyst reduced at 423 K. The spectra show three intense bands located at 1444, 1485, and 1602 cm^{-1} and two weak bands at 1540, 1575, and $\sim$1640 cm^{-1}, in addition to the bands already observed on the support. The bands at 1444 and 1602 cm^{-1} characterize weak Lewis acidic sites while those at 1540 and $\sim$1640 cm^{-1} reveal some Brønsted acidity. The signal at 1485 and 1575 cm^{-1} are common to the various types of acidity present on the surface. Since on silica, pyridine adsorption does not resist an evacuation at 423 K, the bands remaining after such an evacuation can be ascribed to the interaction of the adsorbate with the sulfided phase. It should be noted that on the support the bands at 1455 and 1625 cm^{-1} which characterize the presence of some strong Lewis acidic sites are at least detectable after evacuation at 423 K, while on Ru-based catalyst they are weak but clearly observed. This indicates either the presence of strong Lewis acidic sites on the sulfided phase or a modification of the silica surface composition during the impregnation step. A way to elucidate this point would be to deposit ruthenium on pure silica.

Figure 4 shows the effect of solid reduction on the IR spectra recorded after pyridine evacuation at 423 K. These spectra present the same bands than on Ru/SiO_2 reduced at 473 K, indicating the presence of Brønsted and Lewis (mainly weak) acidity.

The intensity of the Lewis bands increase with the reduction of the Ru-based catalyst up to a reduction temperature of 473 K ($\alpha = 20\%$) while more severe hydrogen treatments provoke a decrease of the acidity. Figure 5 compares the variation of the number of Lewis sites determined from the spectra recorded after a pyridine evacuation at RT and 423 K. In this latter case, pyridine is only adsorbed on the sulfided phase while after evacuation at RT, the band area includes the contribution of the support. However, it has been verified that the latter stays rather constant irrespective of the severity of the pretreatment of the Ru/SiO_2 catalyst, so the observed variation could be related to the sulfided phase. Accordingly, the maximum of Lewis acidic sites is found for the same reduction temperature of ca 473 K, independently of the evacuation temperature. This suggests that reduction of the Ru/SiO_2 catalyst induces a variation of the number of acidic sites rather than a modification of their strength.

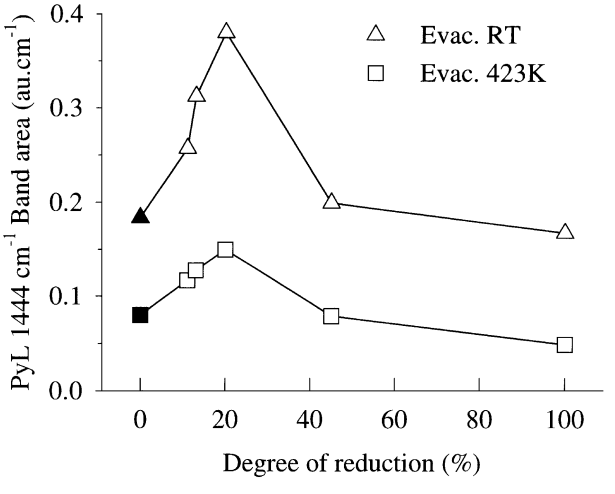

FIG. 5. Variation of the band area characteristic of Lewis acidic sites (1444 cm^{-1}) after pyridine evacuation at room temperature and at 423 K versus the reduction degree of Ru/SiO_2.

The bands related to PyH^+ species are not intense enough to accurately determine the variation of the number of Brønsted acidic sites. However, it should be noticed that the band at 1485 cm^{-1}, which results from pyridine adsorption on both Lewis and Brønsted acidic centers, presents a relatively high intensity. Therefore, the variation of the number of Brønsted acidic sites might be estimated by calculating the ratio between the area of the bands at 1485 cm^{-1} (B + L) and the band at 1444 cm^{-1} (L), which should be proportional to B/L. Figure 6 reports the variation of this ratio (B + L)/L with the degree of reduction and a maximum is also observed for $\alpha = 20\%$ ($T_r = 473$ K). Since the concentration of Lewis acidic sites linearly increases until $\alpha = 20\%$, the increase of (B + L)/L implies an increase of the number of Brønsted acidic sites. For higher reduction degree, the decrease of both L and (B + L)/L provides evidence for a decrease of the number of Brønsted acidic sites. Thus, their variation follows the same trend as that of the Lewis acidic sites.

A similar set of experiments has been performed on the Mo/SiO_2 and $CoMo/SiO_2$ catalysts. Figure 7 reports the IR spectra of the adsorbed pyridine recorded in the 1550–1650 cm^{-1} region. The unpromoted Mo catalyst exhibits mainly an intense band located at 1596 cm^{-1} after evacuation at RT. As mentioned before, this band may be ascribed to weak hydrogen bonded species linked to OH groups of the silica support. After evacuation at 423 K, such an interaction is no longer observed, as the remaining signal presents a low intensity and shifts to 1600 cm^{-1} indicating the presence of a small number of weak Lewis acid sites. On the Co-promoted catalyst and after evacuation at RT, two bands are observed at 1609 and 1598 cm^{-1}, which are still present upon desorption at 423 K. This indicates that the addition of Co to Mo increases the number and the strength of the Lewis sites. However, it is known that on such silica support, Co and Mo sulfides may coexist with the CoMoS phase. Therefore, the resulting acidity modification could indicate the presence of a cobalt sulfide phase. In order to address this problem a similar experiment has been done on a Co/SiO_2. On this solid, pyridine adsorption gives rise to a band at 1601 cm^{-1} (RT evacuation) which shifted to 1606 cm^{-1} upon evacuation at 423 K. Thus, the band observed at 1609 cm^{-1} on the CoMo catalyst could be ascribed to a CoMoS phase which possesses a stronger acidic character than the Mo or Ru supported sulfides. According to these data, the comparison of the strength of Lewis acid sites should be made after pyridine evacuation at 423 K. Figure 8 compares the variation of the concentration

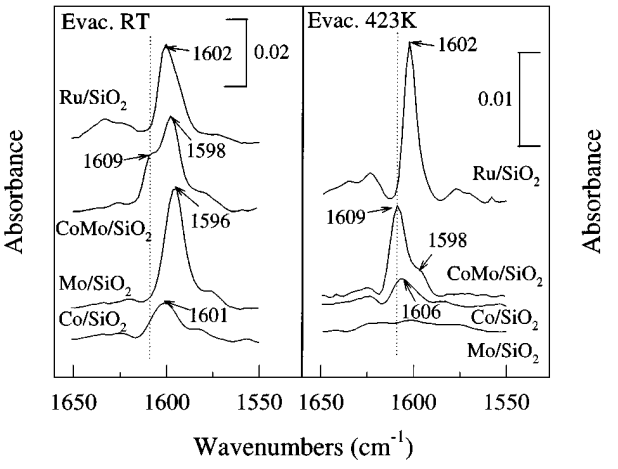

FIG. 7. IR spectra of the ν8a Lewis band of pyridine evacuated at room temperature (left) and at 423 K (right) on the various silica-supported sulfide catalysts (Ru/SiO_2 reduced at 423 K, nonreduced Co/SiO_2, Mo, and $CoMo/SiO_2$ reduced at 573 K).

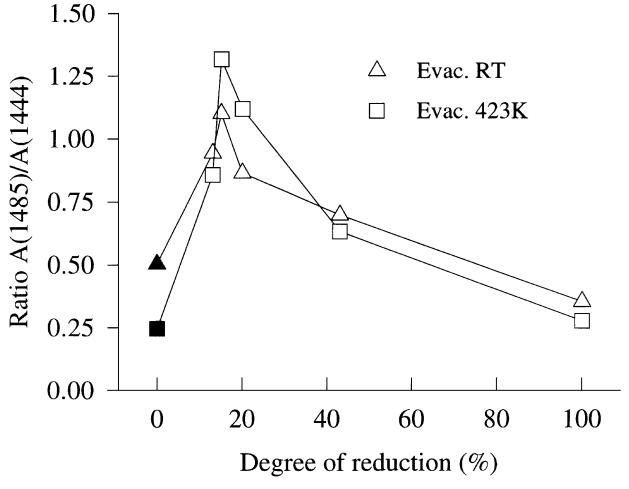

FIG. 6. Variation of the area ratio of the bands at 1485 cm^{-1} over 1444 cm^{-1} after pyridine evacuation at room temperature and at 423 K versus the reduction degree of Ru/SiO_2.

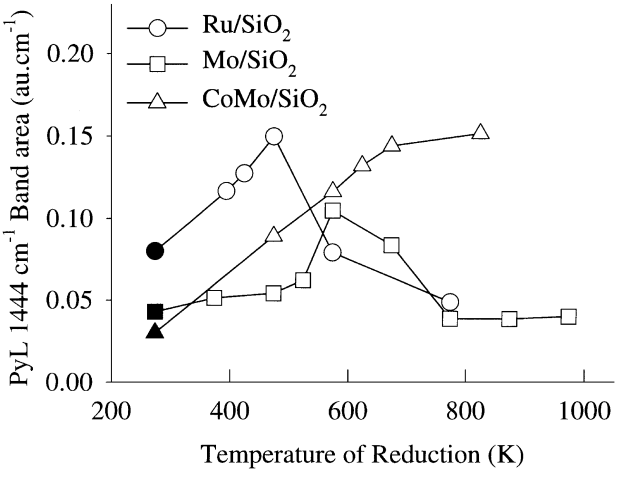

FIG. 8. Variation of the 1444 cm^{-1} band area after pyridine evacuation at 423 K versus the reduction temperature for the three catalysts: Ru/SiO_2, Mo/SiO_2, and $CoMo/SiO_2$.

of Lewis acid sites versus the temperature of reduction for the various systems. The three curves present differences in behavior. As a matter of fact, the Ru catalyst shows a greater number of anionic vacancies for the low temperatures of reduction ($T_r \leq 473$ K) which indicates its higher reducibility than the unpromoted molybdenum catalyst. The addition of promoter to the molybdenum catalyst increases the number of Lewis sites of the sulfided phase whatever the reduction temperature. Furthermore, it gives rise to a continuous growth of the number of sites up to 623 K at which temperature it reaches a plateau, whereas on Mo/SiO_2 the concentration of Lewis acidity is optimum for 573 K. It should also be noted that only weak Brønsted bands are detected on Mo/SiO_2 and $CoMo/SiO_2$ using pyridine as the probe molecule.

Infrared Spectroscopy of Adsorbed 2,6-Dimethylpyridine (Lutidine)

For the Ru catalyst it has been shown that reduction leads to an enhancement of Lewis acidity, but it also creates some Brønsted sites. Nevertheless, the protonic acidity is revealed by relatively weak pyridinium bands. Consequently, in order to confirm the presence of such sites, the adsorption of lutidine, which is more sensitive to weak Brønsted acidity, has been performed. Figure 9 shows the IR spectra of adsorbed lutidine recorded after an evacuation at RT for Ru/SiO_2. In the 1550–1700 cm^{-1} range, four main bands are detected. The two intense bands located at 1583 and 1603 cm^{-1}, whose intensities vary little with the nature of the catalyst pretreatment, correspond to both lutidine adsorbed on Lewis acid sites and to hydrogen-bonded species. The two other bands positioned at 1629 and 1644 cm^{-1} agree fairly well with those reported in the literature for protonated species and they may be respectively ascribed to ν8b and ν8a vibration modes of lutidinium species (40–42). These bands are not present on the silica support treated in the same conditions. According to these data, the number of Brønsted acid sites slightly varies with the degree of reduction of the solid and only a slight maximum emerges for an α value of 12–20% (see also Fig. 10). Figure 10 reports the integrated band areas for two temperatures of lutidine desorption. With respect to a RT lutidine evacuation, a desorption treatment at 423 K reduces the amount of adsorbed species by a constant factor of about 3–4 whatever the S/Ru ratio, indicating that the lutidinium bond strength is not greatly modified. Lutidine has also been adsorbed on unpromoted and promoted molybdenum catalysts. Figure 11

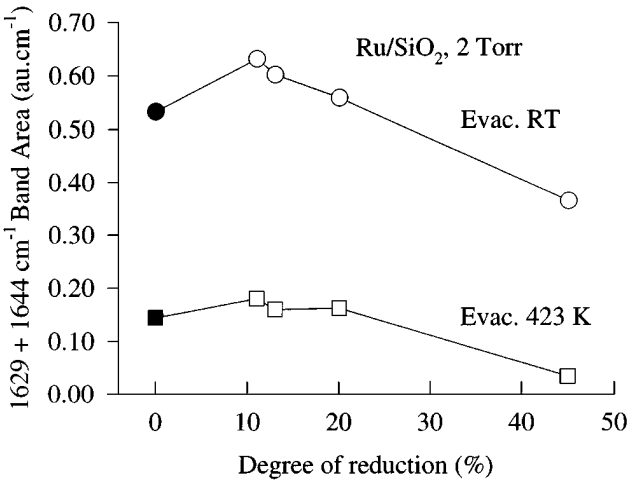

FIG. 10. Variation of the area of the bands characteristic of Brønsted acidic sites (1644 and 1629 cm^{-1}) after 2,6-dimethylpyridine evacuation at room temperature and at 423 K versus the reduction degree of Ru/SiO_2.

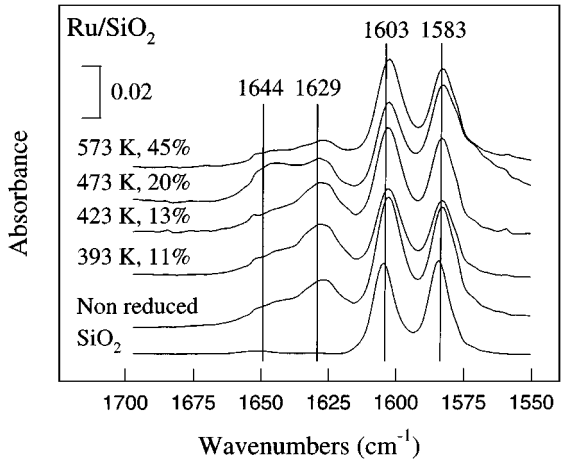

FIG. 9. IR spectra of the species resulting from 2,6-dimethylpyridine (lutidine) evacuation at room temperature on silica and on Ru/SiO_2 reduced at various temperatures.

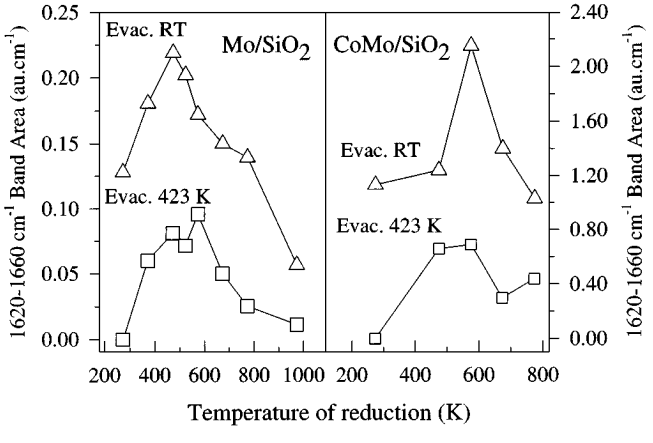

FIG. 11. Variation of the area of the bands characteristic of Brønsted acidic sites (1644 and 1629 cm^{-1}) after 2,6-dimethylpyridine evacuation at room temperature and at 423 K versus the reduction temperature for silica supported unpromoted and Co-promoted molybdenum catalysts.

shows the variations of the ν8a and ν8b lutidinium bands after evacuation at room temperature and at 423 K versus the temperature of reduction. The nonreduced Mo/SiO_2 solid presents also some weak Brønsted acidic sites; all the lutidine desorbs upon evacuation at 423 K. The number of Brønsted acidic sites is modified upon reduction and a net maximum was observed for a reduction temperature of circa 523 K. Therefore, some new SH groups can be created at the surface of Mo/SiO_2 by reducing the catalyst in hydrogen. On this solid, the number of SH groups is about three times lower than over Ru/SiO_2. However, upon evacuation at 423 K, Brønsted band intensities are roughly the same on both catalysts. This suggests that the lutidinium species are more strongly bonded on Mo/SiO_2 than over the ruthenium-based catalyst. The addition of Co to the Mo system gives rise to an important increase of the number of SH groups since about an eightfold increase of band intensities is detected, either after degassing the solid at RT, or at 423 K.

DISCUSSION

The variation of the number of Lewis and Brønsted acid sites induced upon reduction has been investigated over three model silica-supported transition model sulfides: Ru/SiO_2, Mo/SiO_2, and Co-promoted Mo/SiO_2. These catalysts present distinct reactivities and stabilities towards a hydrogen atmosphere leading to different surface properties. These differences may be discussed in terms of the metal–sulfur bond strength, taking into account probe molecule adsorption and temperature-programmed reduction results.

Among the solids studied, the Ru/SiO_2-based catalyst is easily reducible since it could be completely reduced by a hydrogen treatment at 623 K. This treatment allows the formation of coordinatively unsaturated Ru sites. Nevertheless, it is worthwhile noticing that the solid initially possesses enough CUS to give rise to a significant chemisorption of pyridine and lutidine. This chemisorptive ability demonstrates that the surface of the nonreduced material already contains Brønsted and Lewis sites. Their presence is in good agreement with the observed activity towards the transformation of CH_3SH into CH_3SCH_3. As previously reported (31), the S/Ru ratio measured for the nonreduced catalyst is close to 2.7 while the expected value for a fully sulfided Ru crystallite of 3.5 nm may reach 3. This suggests that some surface Ru ions are not in a sixfold coordination state, in agreement with the presence of the observed CUS. In addition to CUS and SH groups, the surface of the nonreduced catalyst may contain bridged S^{2-} (Ru-S-Ru), as well as the S_2^{2-} species belonging to the pyrite RuS_2 structure. Upon hydrogen reduction, some S^{2-}or S_2^{2-} may be in a first step transformed into new SH groups but some SH species may also be released as H_2S. Therefore, the reduction process results in the formation–elimination of SH entities upon reduction which may account for the slight increase of Brønsted acidity up to a degree of reduction of about 20% (Fig. 10). At higher reduction temperatures, surface sulfur depletion induces a decrease of the concentration of anionic species which in turn limit the formation of SH acidic groups leading to a diminution of the overall Brønsted acidity. In the first stages of the reduction, sulfur removal creates some Lewis-type centers that are easily detected using pyridine adsorption. Their number increases up to a reduction temperature of about 473 K (Fig. 5). For higher reduction degrees ($\alpha > 20\%$), the CUS number decreases, although we could expect that sulfur elimination creates more and more CUS, at least in the domain of stability of the sulfided phase ($\alpha \leq 50\%$). This suggests a modification of the Lewis acid site strength due to a change in the sulfur coordination of Ru atoms. However, in such a case, a shift in the ν8a PyL band position would be expected, whereas no detectable modification is observed. Moreover, as shown in Fig. 5, the ratio between the number of PyL evacuated at RT and those evacuated at 423 K is almost constant whatever the temperature of reduction. Another explanation would be that the fraction of surface ruthenium cations presenting a low sulfur coordination is not involved in the pyridine chemisorption process. Current studies using CO as a probe tend to support this assumption since they reveal the presence of Ru cations with various sulfur environments and the appearance of metallic Ru sites which poorly adsorb pyridine at a reduction temperature of 573 K (43). By contrast, molybdenum sulfide never reaches the metallic state in the domain of reduction temperatures investigated in this work.

The similar variation of the activity in CH_3SH condensation and of probe molecule adsorption capacity with the degree of reduction of the solid indicates that acidity is a necessary prerequisite for developing catalytic properties towards this reaction. In a first approach, it could be considered that the sulfide–CH_3SH system behaves similarly to the homologous oxide–alcohol combination, where acidity plays an important role for ether formation (44–48). Taking into account the data obtained in this work, it is, however, difficult to know if both types of acid sites (Brønsted and Lewis) are involved in the catalytic mechanism or if the activity is related to only one particular type. As a matter of fact, a mechanism involving only Brønsted sites is conceivable i.e. the attack of a CH_3SH molecule by a surface proton and the reaction of this species with another CH_3SH molecule. Another way could be a dissociative chemisorption of CH_3SH on a Lewis acidic site (CUS) and a basic anionic sulfur species, leading to the formation of a thiolate species and a new SH group and this latter reacting with another CH_3SH molecule as before. This mechanism is supported by previous work which has shown that CH_3SH dissociatively chemisorbs at the surface of such a catalyst

(31). Moreover, the evolution of a Lewis acid site number not only follows the same trend as the activity but their variation is also in good agreement with activity variation (Figs. 2 and 5). So, we conclude that vacancies-S paired sites are involved in this reaction.

Concerning Mo/SiO_2-based catalysts, this study clearly confirms the effect of cobalt promotion on the reducibility of these solids as previously reported (49, 50). Thus, while only 25% of the sulfur could be removed from the unpromoted Mo/SiO_2 catalyst at high temperature (1073 K), the cobalt-promoted solid could be completely reduced at the same temperature. This difference of reducibility influences to a large extent the variations of acid (Lewis and Brønsted) properties. As shown in Fig. 8, the intensities of PyL bands are lower for the unpromoted molybdenum than for the Co-promoted catalyst, and the variation of the number of Lewis sites with the temperature of reduction is completely different. Indeed, on the unpromoted molybdenum solid, a weak maximum is observed for $T_r = 573$ K, whereas the number of sites increases until a plateau at 673 K on the Co-promoted catalyst is reached. For Mo/SiO_2 despite the relative increase of the particle size in the temperature range 273–673 K (Table 1) the number of CUS created by hydrogen reduction increases, showing the removal of sulfur atoms from the surface. For higher temperatures of reduction, the very low amount of CUS detected may be explained by a significant sintering of the MoS_2 slabs. As for the Co-promoted catalyst, no sintering is observed, explaining probably why no decrease is noted (Table 1). It should be mentioned that the stabilization of the MoS_2 slabs by cobalt has already been reported in the literature (51, 52). Other differences between promoted and unpromoted Mo catalysts concern the strength of the Lewis acid sites: (i) the wavenumber of the ν8a PyL band is shifted upwards in the case of the promoted catalyst (1609 cm^{-1}), whereas its position is respectively observed at 1606 or 1600 cm^{-1} for the Co/SiO_2 and Mo/SiO_2 unicomponent catalysts (Fig. 7); (ii) the intensity of PyL bands remains strong after a vacuum treatment at 423 K for the $CoMo/SiO_2$ and Co/SiO_2 catalyst, whereas it becomes negligible for the Mo/SiO_2 solid. Therefore, the Lewis acidity of the mixed CoMoS phase is stronger than those created on the individual Co and Mo sulfides.

As evidenced by lutidine adsorption, the unpromoted Mo/SiO_2 catalyst presents Brønsted acid sites whose concentration depends on the severity of the reductive treatment. The variation of the concentration of SH species induced by hydrogen is greater than over ruthenium sulfide because, depending on the reduction temperature, a net maximum of SH groups could be observed while on ruthenium sulfide the obtained concentration profile is rather flat with respect to the reduction temperature. Similarly, the interaction of lutidine with the catalyst surface is stronger on Mo/SiO_2 than on Ru/SiO_2 since band intensities are less diminished upon evacuation of the adsorbed species at 423 K. These data indicate that the Mo-SH bonds created on Mo/SiO_2 by hydrogen chemisorption are stronger than those formed on Ru/SiO_2 in similar experimental conditions. This fact could be understood in terms of the metal–sulfur bond strength. The stronger is the M-S bond the lower will be the number of CUS and it might be expected that the more acidic will be the SH groups. These findings agree with a recent work devoted to the understanding of the HDN properties of model TMS (53) in which it was shown that the SH of RuS_2 may act as a nucleophilic moiety, while on MoS_2 they behave more likely as an acidic center (54).

Marked differences in reducibility and acidity between unpromoted and Co-promoted catalysts should be related to the variations in CH_3SH condensation activity. Indeed, the most striking effect is the strongly higher activity, at the optimum, of the cobalt-promoted catalyst, compared to the unpromoted one. However, without hydrogen treatment, the activity for the Co-promoted catalyst is lower than for Mo/SiO_2 (Fig. 2). This could be ascribed to the presence of cobalt above the edges of the MoS_2 slabs, which provides a stabilization effect of the molybdenum sulfide phase upon hydrogen reduction at low temperature (55–58). In the temperature range $T_r = 473$–573 K (Fig. 1), a similar activity is observed for both systems, in agreement with their identical reducibility. In this zone, the created active sites are probably formed by removal of the more labile sulfur anions located on nonpromoted Mo cations. For higher temperatures of reduction (573–723K), the behavior of the two systems splits up. The higher activity of the $CoMo/SiO_2$ is related to the formation of a larger number of CUS due to its greater reducibility and higher stability. Above this temperature ($T_r > 723$ K), a noticeable decrease of the condensation activity occurs. This could be assigned to a beginning of segregation of the CoMoS phase into Co_9S_8 and MoS_2 as indicated by a slope change at this temperature on the TPR curve presented on Fig. 1. Complementary IR experiments using low temperature CO adsorption confirm the occurrence of a segregation at high reduction temperature (43). This process would be responsible for the discrepancy between condensation activity and Lewis sites detected by pyridine, a probe molecule that adsorbs on the different phases present on $CoMo/SiO_2$. This could be assigned to an important diminution of the number of basic sulfur anions leading to a decrease of the number of acid–base couples. This large sulfur depletion induces, also, the beginning of the segregation of the CoMoS phase into Co_9S_8 and MoS_2.

CONCLUSIONS

This study provides evidence for the versatility of the surface properties of sulfide catalysts under reaction

conditions. Indeed, transition metal sulfides are used in hydrotreatment reactions in the presence of several bars of hydrogen and these results point out that the Ru/SiO_2, Mo/SiO_2, and $CoMo/SiO_2$ sulfides present quite a different number of CUS and SH groups, according to the reductive atmosphere. The interest of silica-supported systems which allowed comparison of the acidic properties of various sulfided transition metals by avoiding acidity due to the support should be also underlined. This study also confirms the interest of using 2,6-dimethylpyridine as the probe molecule since it provided evidence of protonic acidity on the sulfided phase at room temperature. Moreover, the reducibility of the solid plays an important role since the lower the strength of the M-S bond, the higher the number of Lewis acid sites and the higher the activity in acid-required reactions. This agrees fairly well with the bond energy model (BEM) based on theoretical calculation of the metal–sulfur bond energies (37, 38). Inversely, the Brønsted character of the SH groups follow an opposite trend because a strong metal–sulfur bond induces a higher protonic character of the SH groups.

This study confirms that the methylmercaptan condensation reaction is an appropriate reaction to characterize acid–base properties of sulfide catalysts since it gives information on such properties even when the number of sites is too low to obtain valuable information by spectroscopic techniques and, also, because it allows the characterization of sulfided catalysts in experimental conditions close to those used in a hydrotreating reaction.

ACKNOWLEDGMENTS

This work was carried out in the framework program of scientific collaboration between France and China. G. Berhault is greatly indebted to the French Ministry of Education for a Ph.D. grant. L. Qu and H. Nie gratefully acknowledge the Association Franco-Chinoise pour la Recherche Scientifique et Technique for financial support.

REFERENCES

1. Tanaka, K., *Adv. Catal.* **33**, 99 (1985).
2. Wambeke, A., Jalowiecki, L., Kasztelan, S., Grimblot, J., and Bonnelle, J. P., *J. Catal.* **109**, 320 (1988).
3. Lacroix, M., Mirodatos, C., Breysse, M., Décamp, T., and Yuan, S., *in* "New Frontiers in Catalysis" (L. Guczi, F. Solymosi, and P. Tétényi, Eds.), p. 597. Elsevier, Budapest, 1993.
4. Joffre, J., Geneste, P., and Lerner, D. A., *J. Catal.* **97**, 543 (1986).
5. Diez, R. P., and Jubert, A. H., *J. Mol. Catal.* **83**, 219 (1993).
6. Zonneyville, H. C., Hoffmann, R., and Harris, S., *Surf. Sci.* **199**, 320 (1988).
7. Gachet, C. G., Dhainaut, E., de Mourgues, L., Candy, J. P., and Fouilloux, P., *Bull. Soc. Chim. Belg.* **90**, 1279 (1981).
8. Pérot, G., *Catal. Today* **10**, 447 (1991).
9. Sundberg, P., Moyes, R. B., and Tomkinson, J., *Bull. Soc. Chim. Belg.* **100**, 967 (1991).
10. Jobic, H., Clugnet, G., Lacroix, M., Yuan, S., Mirodatos, C., and Breysse, M., *J. Am. Chem. Soc.* **115**, 3654 (1993).
11. Komatsu, T., and Hall, W. K., *J. Phys. Chem.* **95**, 9966 (1991).
12. Lacroix, M., Yuan, S., Breysse, M., Dorémieux-Morin, C., and Fraissard, J., *J. Catal.* **138**, 409 (1992).
13. Polz, J., Zeilinger, H., Müller, B., and Knözinger, H., *J. Catal.* **120**, 22 (1989).
14. Topsøe, N. Y., and Topsøe H., *J. Catal.* **139**, 641 (1993).
15. Brunn, L. W., Montagna, A. A., and Paraskos, J. A., *J. Am. Chem. Soc., Div. Petrol. Chem. Prepr.* **21**, 173 (1976).
16. Laine, J., Brito, J., and Yunes, S., *in* "Proceedings, 3rd Int. Conf. on Chemistry and Uses of Molybdenum" (H. F. Barry and P. C. H. Mitchell, Eds.), p. 111. Climax Molybdenum Company, 1979.
17. Parsons, B. I., and Ternan, M., *in* "Proceedings, 6th Int. Cong. Catal., London, 1977" (G. C. Bond, P. B. Wells, and F. C. Tompkins, Eds.), p. 965.
18. Cowley, S. W., and Massoth, F. E., *J. Catal.* **51**, 291 (1978).
19. Ratnasamy, R., and Knözinger, H., *J. Catal.* **54**, 155 (1978).
20. Kung, M. C., and Kung, H. H., *Catal. Rev-Sci. Eng.* **27**(3), 425 (1985).
21. Knözinger, H., *Adv. Catal.* **25**, 184 (1976).
22. Topsøe, N. Y., Topsøe, H., and Massoth, F. E., *J. Catal.* **119**, 252 (1989).
23. Miciukiewicz, J., Zmierczak, W., and Massoth, F. E., *in* "Proceedings, 8th Int. Cong. Catal.," Vol. 2, p. 671. Verlag Chemie, Weinheim, 1984.
24. Lee, H. C., and Butt, J. B., *J. Catal.* **49**, 320 (1977).
25. Knözinger, H., and Ratnasamy, P., *Catal. Rev. Sci. Eng.* **17**, 31 (1978).
26. Bensitel, M., Saur, O., and Lavalley, J. C., *Mater. Chem. Phys.* **28**, 309 (1991).
27. Knözinger, H., Bühl, H., and Ress, E., *J. Catal.* **12**, 121 (1968).
28. Sugioka, M., Kamanaka, T., and Aomura, K., *J. Catal.* **52**, 531 (1978).
29. Mashkina, A. V., Grunvald, V. R., Nasteka, V. I., Borodin, B. P., Yakovleva, V. N., and Khairulina, L. N., *React. Kinet. Catal. Lett.* **41**, 357 (1990).
30. Saur, O., Chevreau, T., Lamotte, J., and Lavalley, J. C., *J. Chem. Soc. Faraday Trans. I* **77**, 427 (1981).
31. Berhault, G., Lacroix, M., Breysse, M., Maugé, F., Lavalley, J-C., and Qu, L. L., *J. Catal.* **170**, 37 (1997).
32. Pecoraro, T. A., and Chianelli, R. R., *J. Catal.* **67**, 430 (1981).
33. Lacroix, M., Boutarfa, N., Guillard, C., Vrinat, M., and Breysse, M., *J. Catal.* **120**, 473 (1989).
34. Ledoux, J., Michaux, O., Agostini, J., and Panissod, P. J., *J. Catal.* **102**, 275 (1986).
35. Vissers, P. R., Groot, C. K., van Oers, E. M., De Beer, V. J. H., and Prins, R., *Bull. Soc. Chim. Belg.* **93**, 813 (1984).
36. Topsøe, H., Clausen, B. S., Topsøe, N-Y., Hyldtoft, J., and Nørskov, J. K., *J. Am. Chem. Soc., Div. Petrol. Chem. Prepr.* **38**, 638 (1993).
37. Nørskov, J. K., Clausen, B. S., and Tøpsoe, H., *Catal. Lett.* **13**, 1 (1992).
38. Toulhoat, H., and Kresse, G., *J. Am. Chem. Soc., Div. Petrol. Chem. Prepr.* **42**, 114 (1997).
39. Knop, O., *Canad. J. Chem.* **41**, 1838 (1963).
40. Jacobs, P. A., and Heylen, C. F., *J. Catal.* **34**, 267 (1974).
41. Dewing, J., Monks, G. T., and Youll, B., *J. Catal.* **44**, 226 (1976).
42. Matulewicz, E. R. A., Kerkhof, F. P. J. M., Moulijn, J. A., and Reitsma, H. J., *J. Colloïd Interface Sci.* **77**, 110 (1980).
43. Berhault, G., Lacroix, M., Breysse, M., Maugé, F., Lavalley, J-C., and Qu, L. L., to be published.
44. DeCanio, E. C., Nero, V. P., and Bruno, J. W., *J. Catal.* **135**, 444 (1992).
45. Davis, B. H., *in* "Adsorption and Catalysis on Oxide Surface" (M. Che and G. C. Bond, Eds.), p. 309. Elsevier, Amsterdam, 1985.
46. Yamaguchi, T., and Tanabe, K., *Bull. Chem. Soc. Jpn.* **47**, 424 (1974).
47. Matsushima, T., and White, J. M., *J. Catal.* **44**, 183 (1976).
48. Bandiera, J., and Naccache, C., *Appl. Catal.* **69**, 139 (1991).

49. Topsøe, H., Clausen, B. S., Topsøe, N-Y., Nørskov, J. K., Ovesen, C. J., and Jacobsen, C. J. H., *Bull. Soc. Chim. Belg.* **104**, 283 (1995).
50. Nag, N. K., Fraenkel, D., Moulijn, J. A., and Gates, B. C., *J. Catal.* **66**, 162 (1980).
51. Vrinat, M., and de Mourgues, L., *Appl. Catal.* **5**, 43 (1983).
52. Prins, R., De Beer, V. J. H., and Somorjai, G., *Catal. Rev. Sci. Eng.* **31**, 1 (1989).
53. Thomas, C., Vivier, L., Lemberton, J-L., Kasztelan, S., and Pérot, G., *J. Catal.* **167**, 1 (1997).
54. Cattenot, M., Portefaix, J. L., Afonso, J., Breysse, M., Lacroix, M., and Pérot, G., *J. Catal.* **173**, 366 (1998).
55. Topsøe, H., Candia, R., Topsøe, N-Y., and Clausen, B. S., *Bull. Soc. Chim. Belg.* **93**, 783 (1984).
56. Topsøe, H., and Clausen, B. S., *Catal. Rev. Sci. Eng.* **26**, 395 (1984).
57. Topsøe, H., Clausen, B. S., Candia, R., Wivel, C., and Mørup, S., *Bull. Soc. Chim. Belg.* **90**, 1189 (1981).
58. Topsøe, N-Y., and Topsøe, H., *J. Catal.* **84**, 386 (1983).